Effect of Signal Alteration on Learning Shape Identity using Sparse Representations

Michael Slugocki (slugocm@mcmcaster.ca)[1] **Allison B. Sekuler (sekuler@mcmcaster.ca)**[1,2,3]
Patrick J. Bennett (bennett@mcmaster.ca)[1]

[1] Department of Psychology, Neuroscience & Behaviour, McMaster University
[2] Rotman Institute, Baycrest Health Sciences
[3] Department of Psychology, University of Toronto

Abstract

The primate visual system constructs intermediate shape representations using something akin to a radial modulation function (Pasupathy & Connor, 2001, 2002). However, less is known about whether sparse representations derived from radial modulation functions are useful in performing higher level tasks, such as object recognition. The current study investigated whether several shape-encoding schemes based on radial modulation functions can be used by neural networks to learn the identity of closed-contour shapes degraded by various amounts of blur or curvature noise. We measured performance of neural networks on a shape classification task with 10 sets of 10 unique shape classes, each consisting of 10,000 samples. When the shapes were not degraded, classification accuracy for representations based upon the radial position of, or angularity between, either positive or negative curvature extrema was high. When the shapes were blurred, classification accuracy was significantly lower for representations based on the angles between curvature extrema. However, adding frequency noise reduced classification accuracy by similar amounts across sparse representation types. Sparse representations also led to faster training of neural networks compared to richer representations. We conclude that sparse shape vectors derived from radial functions can support shape identification, and faster training of networks for shape identity.

Keywords: Shape encoding, Form perception, Neural networks

Introduction

The human visual system is highly sensitive to changes in curvature along the outline contour of objects (Wilkinson, Wilson, & Habak, 1998; Hess, Wang, & Dakin, 1999; Jeffrey, Wang, & Birch, 2002). Such heightened sensitivity to curvature has been attributed to the polar-based coding scheme used by primate visual cortex to encode shape (Poirier & Wilson, 2006). Physiological data on response properties of V4 neurons provide support for a polar-based coding scheme, in which V4 neurons respond to curvature extrema relative to the center of a visual stimulus (Pasupathy & Connor, 2001, 2002). From this population code, a radial modulation function mapping changes in curvature across polar angle can be extracted to represent the outline of an object (Pasupathy & Connor, 2001).

Several investigators have proposed that intermediate visual areas represent the outline shape of objects using sparse coding schemes based either on the radial position of curvature extrema (Pasupathy & Connor, 2001, 2002; Poirier & Wilson, 2006; Carlson, Rasquinha, Zhang, & Connor, 2011), or the angular separation between curvature extrema (Cadieu et al., 2007; Dickinson, Bell, & Badcock, 2013; Schmidtmann, Jennings, & Kingdom, 2015). Sparse coding of shape boundary is important to understand, as sparser neural responses are computationally efficient (Carlson et al., 2011), require less metabolic energy to process (Levy & Baxter, 1996), and can improve storage capacity (Treves & Rolls, 1991). Most models of shape encoding are concerned with accurate shape reconstruction of stimuli from neural responses (Pasupathy & Connor, 2001, 2002; Carlson et al., 2011), rather than examining whether these codes can be used to classify shapes into categories based on contour boundary. Certainly, issues arising from signal degradation and additions of noise could pose problems in using such sparse coding strategies in linking form with identity.

Therefore, to test whether sparse shape vectors can be used to learn to identify shapes, we trained an MLP neural network on different sets of custom generated shapes, either with or without signal degradation, and compared performance of the neural network across different representation types.

Methods

Sets of shapes were constructed using Radial Frequency (RF) contours (see Wilkinson et al., 1998, for original equation) defined by:

$$r(\theta) = \bar{r}(1 + A_1 sin(\omega_1\theta + \phi_1) + A_2 sin(\omega_2\theta + \phi_2) + A_3 sin(\omega_3\theta + \phi_3)) \quad (1)$$

where θ is the polar angle, $\bar{r}$ is the mean radius of the shape, and the modulation amplitude, radial frequency, and phase of the two RF components are represented by A_i, ω_i, and ϕ_i, respectively. To avoid having a contour cross the center of the pattern, the total modulation amplitude summed across all three RF components (i.e., $A_1 + A_2 + A_3$) never exceeded 0.99.

In total, 10 sets of shapes, each comprised of 10 unique shape families, were generated (see Figure 1). A shape family was generated by choosing a unique three-dimensional vector of radial frequencies ($\vec{\omega}$ with components between 0 - 9

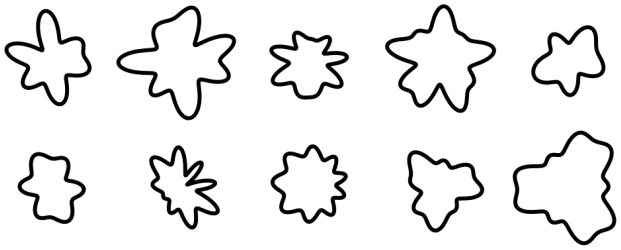

Figure 1: Example of one set of shapes used in the current study. Each shape is one sample from a different shape family. Each set consisted of 10 shape families, and each shape family consisted of 10,000 samples. A total of 10 sets of shape families were generated.

cycles/2π) that was never repeated within the shape set. However, we allowed for $\vec{r}$, amplitudes ($\vec{A}$)), and relative phi ($\vec{\phi}$)) to vary across samples within a family: each shape family was comprised of 10,000 samples. Ten shape classes were generated per set using these constraints, for a total of 1,000,000 shapes.

The various shape representations (vectors) used to train MLP networks are shown in Figure 2. Two different sparse

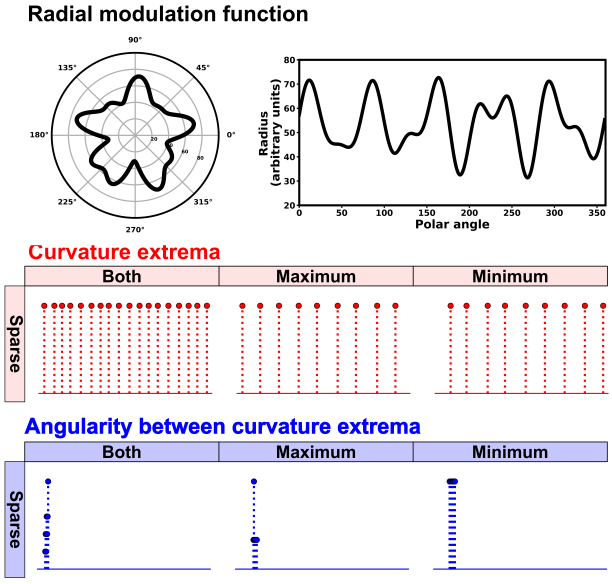

Figure 2: *Top-left*: Radial modulation function of a single shape plotted in polar coordinates. *Top-right*: Plot of radial modulation as a function of polar angle for shape sample shown on left. *Bottom-left*: Visualization of sparse representations based on polar angle of curvature extrema from radial modulation displayed above. *Bottom-right*: Visualization of sparse representations of angular separation between curvature extrema. Note that values along abscissa do not correspond to same values.

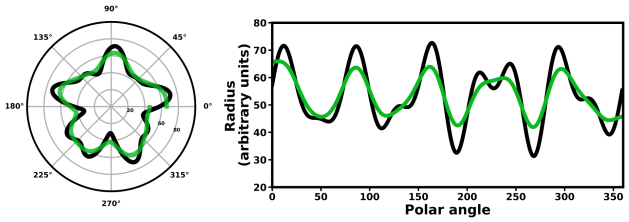

Figure 3: *Left*: Polar plot of unaltered radial modulation function (black) and the same representation after Gaussian smoothing (σ = 5) has been applied to the function (green). *Right*: Radial modulation of unaltered and smoothed representation as a function of the polar angle in degrees.

shape representations were derived from radial modulation functions for each shape (shown in black), one representation was based on the location of curvature extrema (shown in red), and the other was based on the angular separation between these extrema (shown in blue).

Experiment 1: Signal degradation

To simulate signal degradation and general smoothing that may arise from visual processing, we applied various degrees of Gaussian blurring to sparse radial modulation representations, and then recomputed all sparse representations using these new, blurred stimuli (see Figure 3).

Experiment 2: Curvature noise

To examine how the addition of curvature noise affects performance across shape representations, we added an irrelevant, fourth RF component to each original shape vector. The frequency of this component was either absent, low (ω_4: 1-5), medium (ω_4: 6-11), or high (ω_4: 12-16). Because the sum of amplitudes across RF components was restricted to values less or equal to 0.99, the amplitude of this fourth component (A_4) was allowed to take any value between 0 and (0.99 - $(A_1 + A_2 + A_3)$). The phase was set to a random value across samples. An illustration of each frequency noise in different ranges is displayed in Figure 4.

ML network architecture and training

A 3-layer MLP network was trained and tested on shape representations (Figure 5). This neural network architecture was chosen because preliminary simulations demonstrated that this network yielded best classification performance on non-altered shape representations compared to deeper MLP networks (i.e. > 3 layers) and CNNs of varying depth (3-6). Dropout was also present between dense layers to promote regularization, and was set to a value of 0.3.

Results

Experiment 1: Signal smoothing

Results from Experiment 1 are shown in Figure 6, which plots classification accuracy for sparse shape vectors plotted as a

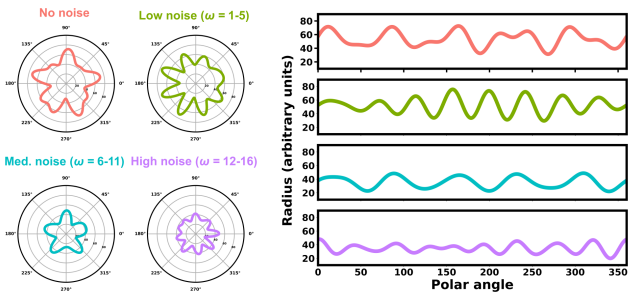

Figure 4: Plots demonstrating RF noise conditions where the noise RF component added to original shape could be low, medium, or high frequency.

function of blur. Classification accuracy was generally high across all representations tested. However, performance was better, and more robust to signal smoothing, for sparse vectors encoding curvature extrema as a function of polar angle compared to vectors encoding angular separation between curvature extrema. Classification based on sparser representations of shape outlines (i.e, based on only max or min curvature extrema) were also more robust to signal smoothing as compared to less efficient codes. However, this result was observed only when curvature extrema were coded as a function of polar angle, and the exact opposite relation was observed for codes based on angularity between curvature extrema.

Experiment 2: Curvature noise

Results from Experiment 2 are shown in Figure 7. Classification accuracy was highest for networks trained and tested with noise-absent shape representations. Furthermore, the addition of curvature noise had no noticeable effect on the classification performance for networks trained and tested with non-

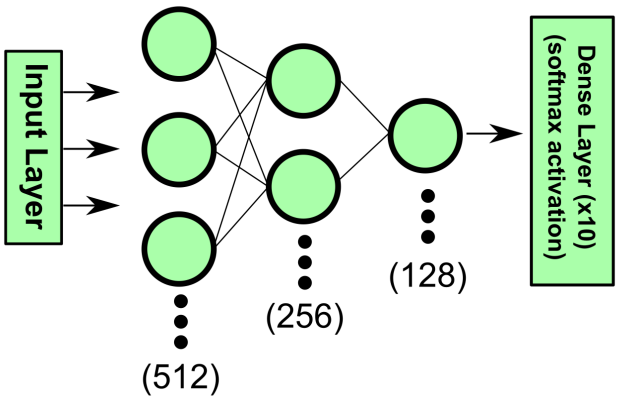

Figure 5: Schematic of MLP architecture used. Dropout layers were omitted from schematic for clarity, but were present between all dense layers of the network.

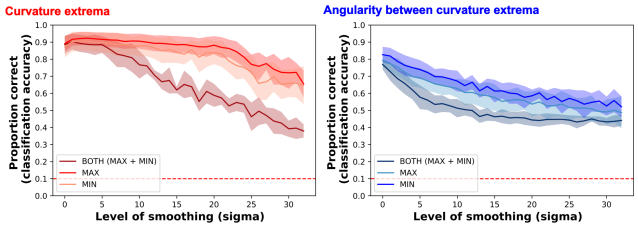

Figure 6: *Left*: Classification accuracy plotted as a function of level of signal blurring (σ) for representations based on encoding of curvature extrema at different polar angles, with colour indicating what curvature extrema were used when generating representations. *Right*: Abscissa and ordinate are same as in left figure, except plot shows performance for networks trained and tested on shape vectors based on angular separation between extrema.

sparse radial modulation functions, regardless of the noise frequency.

In contrast, the frequency of the noise RF component had a large effect on classification performance of networks that were trained and tested with sparse representations based solely on curvature extrema. Specifically, high frequency RF noise components caused large declines in classification accuracy compared to noise RF components of relatively lower frequency. Furthermore, performance was better for shape

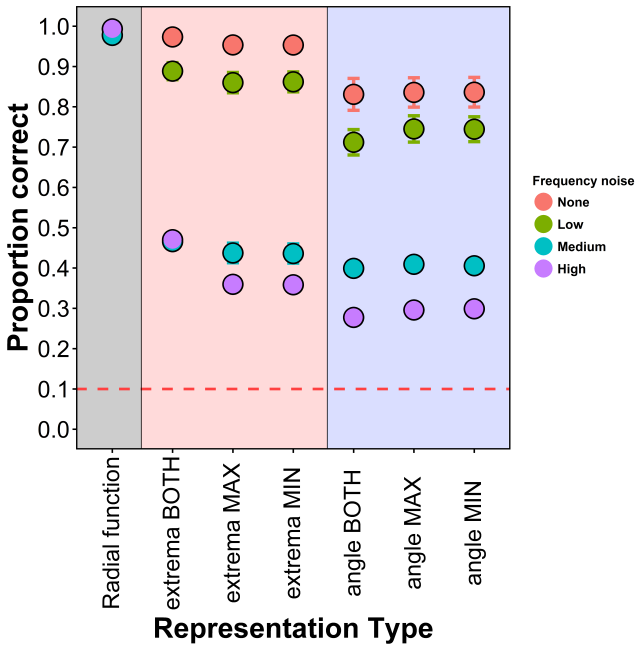

Figure 7: Classification performance of MLP networks trained and tested across different types of shape representations. The colour of each point indicates the level of frequency noise added to original vectors.

representations that coded the polar angles of curvature extrema rather than the angles between extrema. Sparsity of codes within a representation type (i.e., curvature by polar angle), had little effect over classification accuracy.

Discussion

These simulations demonstrate that extremely sparse shape representations can be used to classify outline shapes composed of three radial frequencies, but that classification accuracy can be affected, sometimes drastically, by signal blur and RF noise.

A surprising result was observed in Experiment 2, as classification accuracy declined dramatically when irrelevant higher frequencies, but not lower frequencies, were added to radial representations of shape identity. This result stands in contrast to psychophysical data that suggests the human visual system represents radial frequencies between approximately 3 - 10 cycles/2π (Habak, Wilkinson, Zakher, & Wilson, 2004; Bell, Badcock, Wilson, & Wilkinson, 2007; Bell & Badcock, 2009; Bell, Wilkinson, Wilson, Loffler, & Badcock, 2009), and that human observers are most sensitive to noise occurring at lower spatial frequencies (Bell et al., 2007; Bell & Badcock, 2009). Furthermore, these results demonstrate that the types of noise human observers are sensitive to when discriminating shapes differs dramatically from the types of noise which most affects performance of neural networks using similar shape representations. Perhaps, higher visual areas are applying low-pass filters to attenuate the effect high frequency noise has in using sparse representation to code for shape identity. Although our results are consistent with this idea, more direct tests aimed at evaluating this hypothesis are needed.

In summary, our results support neurophysiological evidence suggesting sparse coding of shape boundaries based on curvature extrema is a viable transformation that still retains useful information that can be used to classify shapes despite its sparseness. Given our findings, we conclude sparse vectors can be used as a viable coding strategy in linking form with identity, although it is unclear how these results may extend under more complex circumstances.

Acknowledgments

Financial support was provided by Discovery Grants to A.B. Sekuler and P.J. Bennett from the Natural Sciences and Engineering Research Council of Canada (NSERC).

References

Bell, J., & Badcock, D. R. (2009, March). Narrow-band radial frequency shape channels revealed by sub-threshold summation. *Vision Research*, *49*(8), 843-50.

Bell, J., Badcock, D. R., Wilson, H., & Wilkinson, F. (2007, May). Detection of shape in radial frequency contours: independence of local and global form information. *Vision Research*, *47*(11), 1518-22.

Bell, J., Wilkinson, F., Wilson, H. R., Loffler, G., & Badcock, D. R. (2009, September). Radial frequency adaptation reveals interacting contour shape channels. *Vision Research*, *49*(18), 2306-17.

Cadieu, C., Kouh, M., Pasupathy, A., Connor, C. E., Riesenhuber, M., & Poggio, T. (2007, September). A Model of V4 Shape Selectivity and Invariance. *Journal of Neurophysiology*, *98*(3), 1733–1750.

Carlson, E. T., Rasquinha, R. J., Zhang, K., & Connor, C. E. (2011, February). A Sparse Object Coding Scheme in Area V4. *Current Biology*, *21*(4), 288–293.

Dickinson, J. E., Bell, J., & Badcock, D. R. (2013, May). Near their thresholds for detection, shapes are discriminated by the angular separation of their corners. *PLoS ONE*, *8*(5), 1-9.

Habak, C., Wilkinson, F., Zakher, B., & Wilson, H. R. (2004, November). Curvature population coding for complex shapes in human vision. *Vision Research*, *44*(24), 2815-23. doi: 10.1016/j.visres.2004.06.019

Hess, R. F., Wang, Y. Z., & Dakin, S. C. (1999, Oct). Are judgements of circularity local or global? *Vision Research*, *39*(26), 4354-60.

Jeffrey, B. G., Wang, Y. Z., & Birch, E. E. (2002, Nov). Circular contour frequency in shape discrimination. *Vision Res*, *42*(25), 2773-9.

Levy, W. B., & Baxter, R. A. (1996, April). Energy Efficient Neural Codes. *Neural Computation*, *8*(3), 531–543.

Pasupathy, A., & Connor, C. E. (2001). Shape representation in area V4: Position-specific tuning for boundary conformation. *Journal of Neurophysiology*, *86*(5), 2505–2519.

Pasupathy, A., & Connor, C. E. (2002, December). Population coding of shape in area V4. *Nature Neuroscience*, *5*(12), 1332—1338.

Poirier, F. J., & Wilson, H. R. (2006). A biologically plausible model of human radial frequency perception. *Vision Research*, *46*(15), 2443 - 2455.

Schmidtmann, G., Jennings, B. J., & Kingdom, F. A. A. (2015, November). Shape recognition: convexities, concavities and things in between. *Scientific Reports*, *5*, 17142.

Treves, A., & Rolls, E. T. (1991, January). What determines the capacity of autoassociative memories in the brain? *Network: Computation in Neural Systems*, *2*(4), 371–397.

Wilkinson, F., Wilson, H. R., & Habak, C. (1998, November). Detection and recognition of radial frequency patterns. *Vision Research*, *38*(22), 3555-68.